Paper 44

Resultant-Magnetization Based Magnetic Field Interpretation

Foss, C.A. [1]

1. CSIRO Mineral Resources, North Ryde, Sydney, Australia

ABSTRACT

Magnetic field inversion allowing freedom in direction of magnetization has become much more widely used lately, despite having only recently been considered impractical or at best unreliable. Uncertainty in direction of magnetization which drives the requirement for this capability arises from the contribution to the magnetization of a rock from remanent magnetization oriented in an unknown direction. The scalar Koenigsberger ratio of the strength of remanent to induced magnetization is insufficient to characterize this vector relationship, and I suggest that this be supplemented with the apparent resultant rotation angle (ARRA), which is a measure of difference between the local geomagnetic field and resultant (total) magnetization direction. I present case studies which show that for well-defined and well-isolated compact anomalies, there is considerable stability of estimated magnetization direction. A case study of a more complex distribution of multiple magnetizations illustrates that complexity can be managed with user-guided inversion. I suggest that some rotation of magnetization away from the present field direction is the norm rather than a special case, and that most magnetic field inversion studies would benefit from at least inspection and consideration of an optimum magnetization direction solution in addition to standard induced-magnetization-only solutions that are commonly generated. Recovery of magnetization direction from magnetic field analysis or inversion is strongly dependent on the distribution of magnetization, with elongate sheets posing particular difficulties. This study shows that inversions are capable of recovering consistent estimates of magnetization direction, regardless of shape detail for elongations of up to six times the closest approach of measurement.

INTRODUCTION

The external magnetic field generated by a body of magnetization is a function of the magnetization intensity, orientation, and its spatial distribution. As shown in Figure 1, the magnetization of any incremental element of the body is the vector resultant of remanent and induced components, the amplitude ratio of which is known as the Koenigsberger ratio or 'Q factor'.

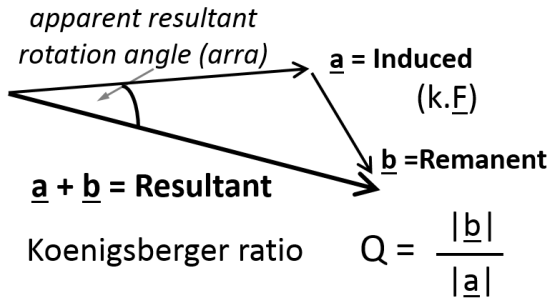

Figure 1: Resultant (or 'total') magnetization is the vector sum of induced and remanent components

The magnetization of a rock with low Koenigsberger ratio (e.g. < 0.2) is close to that of the local geomagnetic field (except in extreme circumstances where it is rotated by substantial anisotropy of magnetic susceptibility or self-demagnetization). The converse that a moderate to high Koenigsberger ratio magnetization (e.g. > 0.5) is rotated from the local geomagnetic field direction is not necessarily true. The remanent magnetization may itself have a direction close to that of the local geomagnetic field (Macnae, 1994), which is commonly the case for 'viscous' remanent magnetizations carried by multi-domain magnetite, however there are also intense 'hard' remanent magnetizations, such as those carried by lamellar magnetism (McEnroe et al., 2016). The scalar Koenigsberger ratio is insufficient to describe the vector rotation of resultant magnetization, and should be augmented by the 'apparent resultant rotation angle' (ARRA), which is the angle between the resultant magnetization and the local geomagnetic field. Resolution of induced and remanent magnetization is only possible if the magnetic susceptibility or Koenigsberger ratio are provided independently. Since remanent and induced components of magnetization are not individually resolved by a magnetic field inversion, it seems sensible to invert for their resultant (also known as 'total' magnetization), and investigate their separation subsequently. This vector separation is non-unique and interpretive. Correct determination of resultant magnetization direction is crucial for magnetic field interpretation. Modelling or inversion with an incorrect magnetization direction gives erroneous estimates of location and structural dip for that magnetized body. Recovered estimates of magnetization direction may carry geological information about the age of acquisition of the magnetization and the influence of any subsequent tectonic rotations, and the resultant magnetization direction is also required for transforms such as reduction to pole (RTP).

There is a wide range of methods to estimate source magnetization from analysis of magnetic field data. Helbig analysis can be applied (Helbig, 1963; Schmidt and Clark; 1998,

In "Proceedings of Exploration 17: Sixth Decennial International Conference on Mineral Exploration" edited by V. Tschirhart and M.D. Thomas, 2017, p. 637–648

Phillips, 2005; Phillips et al. 2007; Foss and McKenzie, 2011). Cross-correlation of RTP, which has high sensitivity to magnetization direction, with the total gradient, which has low sensitivity to magnetization direction, is the basis of several methods of estimating magnetization direction (e.g. Roest et al. 1992; Roest and Pilkington, 1993; Fedi et al. 1994; Dannemiller and Li, 2006). Eigen vector analysis and normalized source strength are the basis for several other approaches (Clark, 2012, 2013; Beiki et al. 2012; Pilkington and Beiki, 2013). A comprehensive review of methods to recover source magnetization direction from magnetic field data is provided by Clark (2014). Inversion of magnetic field data while solving for magnetization direction has been addressed using both parametric algorithms (e.g. Foss, 2006; Foss and McKenzie 2009; Pratt et al. 2014) and voxel algorithms (e.g. Lelièvre and Oldenburg, 2009; Li et al. 2010; Li 2012; Ellis et al. 2012, Macleod et al. 2013; Fullagar and Pears, 2015), while Paine et al. (2001) applied inversion to derive the spatial distribution of magnetization from data transforms insensitive to magnetization direction. In this paper I present results of parametric inversion, but because (as I shall show) shape has only minor influence on the magnetic field expression of compact sources, the conclusions are equally relevant for voxel inversions.

Forward computation of magnetic fields for specified combinations of remanent and induced magnetizations is straightforward. However, the inverse problem of solving for a magnetization and its distribution from given magnetic field data is fundamentally non-unique, even if the direction of that magnetization is known or correctly assumed. Fortunately the scope of non-uniqueness is substantially reduced by assumptions (which in individual cases may or may not be geologically justifiable) that a magnetization is homogeneous and compact. The specific challenge of how an unknown direction of magnetization reduces confidence in inversion depends on the spatial distribution of that magnetization. A thin sheet '2D' magnetization has no sensitivity to any component of magnetization parallel to the strike of the sheet. Furthermore, the structural dip of the sheet and apparent inclination of magnetization in the plane perpendicular to it combine into a single term from which they cannot be individually resolved. There is therefore limited information on magnetization that can be recovered from the magnetic anomaly of an extensive planar sheet. For a dipole source however, Helbig (1963) established that magnetization direction can be uniquely resolved by analysis of the magnetic field measured across a horizontal plane (provided the horizontal center of magnetization is known). The fundamental difference in ability to recover magnetization direction from 2D and compact magnetizations is obviously critical to modelling and inversion studies. Commonly used classification of forward modelling routines as being '2D' or '3D' is not sufficient for studies which must recover magnetization estimates. A more suitable classification, based on data distribution, is 'profile' or 'full anomaly' modelling or inversion, with full anomaly studies required to recover the 3D magnetization vector (some compensation for spatial restriction of measurements to a single profile can be obtained by measurement of multiple field components or gradient elements along that profile).

The simplest forms of inversion proceed by successively searching for solutions of reduced data misfit. If a solution is known to have been found from an exhaustive search of multi-parameter space, then that model is by definition the best combination of parameter values. The truth of this model in representing the subsurface magnetization depends on the validity of the assumptions of the model, and the fidelity and sufficiency of the data. If the data misfit increases sharply for all variation of parameters away from the optimum solution, there is a high sensitivity in defining the model (without assurance that the model is correct). If there is only a slight increase of data misfit away from the optimum solution, so that the location of that minimum is susceptible to displacement by small data imperfections and mismatches, then the model solution has only low sensitivity.

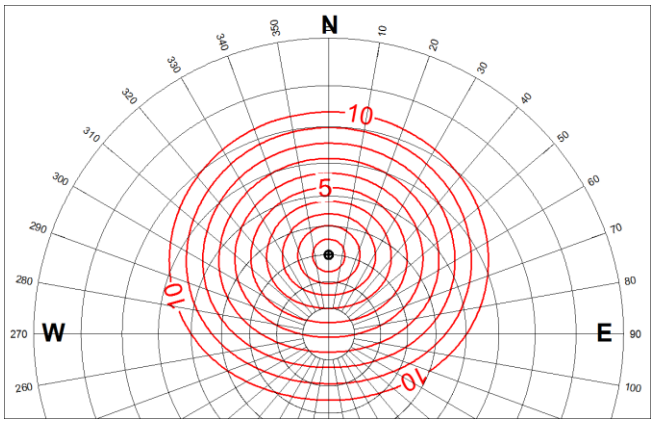

Figure 2: Normalized misfit for the TMI field of identical moment, co-located dipoles, one having a dipole of declination 0, inclination -60).

Figure 2 shows an empirical test of Helbig's assertion that magnetization direction can be estimated from the magnetic field expression of a dipole of known horizontal location. This figure plots the contoured normalized least-squares misfit (rms misfit divided by input data rms) between the magnetic field due to a dipole of specified magnetization direction and co-located dipoles of other test directions. The misfit increases smoothly and uniformly for all displacements away from the correct direction. Reduction of that misfit value is the driving force of an inversion, and smooth convergence towards a minimum as mapped in Figure 2 indicates that an inversion from any starting point within the contoured space should reliably converge to that direction.

Magnetization intensity and direction values derived from magnetic field inversion are the best estimates of the volumetric vector sum of all magnetizations in that source, with some preferential weighting of the shallower magnetizations. High variability of magnetization across a wide range of scales means that this average magnetization may not exist as a discrete magnetization at any point. Hopefully, however, a comprehensive sampling of induced and remanent magnetizations should confirm that average estimate (as is shown in a case study by Austin and Foss, 2014). Fortunately, many geological bodies have magnetizations which vary about a meaningful average value, and in some cases magnetizations

estimated from magnetic field interpretation agree with even sparse palaeomagnetic sampling. This is shown, for instance, by the many magnetic field studies of the Black Hill Norite (Schmidt and Clark, 1997; Phillips 2005; Foss and McKenzie 2011; MacLeod and Ellis 2013; Pratt et al. 2014) which yield magnetization estimates in good agreement with the limited palaeomagnetic sampling (Schmidt et al. 1993; Rajagopalan et al 1993), even though most of those magnetization estimates are made on a body adjacent to that sampled in the palaeomagnetic study.

A CASE STUDY INVERSION OF AN ANOMALY DUE TO REMANENT MAGNETIZATION

Figure 2 illustrates the trivial case for inversion where direction of magnetization is the only unknown model parameter to be solved. The caveats of Helbig's analysis that it applies strictly to a dipole source of known horizontal location suggest that a practical test of inversion to recover magnetization direction should also solve for unknown location and shape of a magnetization. Furthermore, Helbig analysis applies to the field of a dipole, whereas practical field interpretation requires separation of the field ascribed to any source from the background regional field (and from any other overlapping fields of other sources).

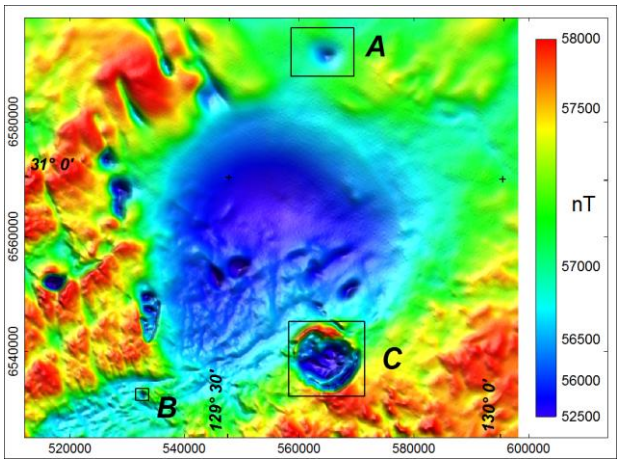

Figure 3: TMI image of the Coompana area.

Figure 3 shows total magnetic intensity (TMI) over the southwestern section of the 2015 Coompana airborne magnetic and radiometric survey flown for the Geological Survey of South Australia (Heath et al., 2015). The local geomagnetic field has an inclination of -63° and declination of +13°. The magnetic field variation is dominated by a 2000 nT negative anomaly of 50 km diameter. There are also multiple smaller anomalies around and superimposed on the main anomaly (Foss et al., 2016a).

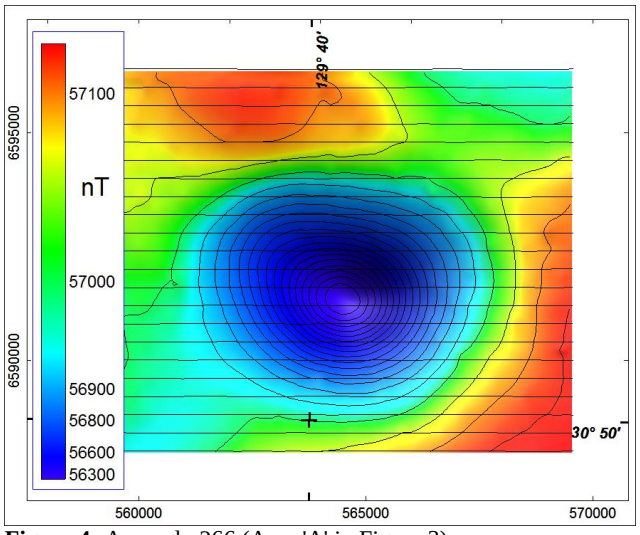

Figure 4: Anomaly 266 (Area 'A' in Figure 3).

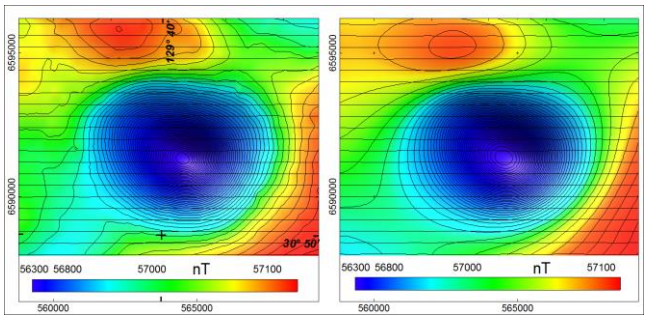

Figure 5: Anomaly 266 measured TMI (left) and computed (right).

A satellite anomaly to the north (anomaly 266 in the Australian Remanent Anomalies Database) shown as area 'A' in Figure 3 is imaged in greater detail in Figure 4. This is a substantial anomaly in its own right, with an amplitude of 900 nT and a diameter of 7 km. This anomaly has been inverted using parametric inversion in ModelVision. Total magnetic intensity forward computed from the final inversion model is compared with measured TMI in Figure 5. The inversion clearly provides an excellent match to the input measured field (but precision of fit does not assure correctness of the model). The model was generated by fitting a smooth (2^{nd} order polynomial) surface to the data surrounding the anomaly, as an estimate of the background field which would be expected in the absence of the anomalous magnetization, and then running an inversion using the model of an elliptic-section pipe with horizontal top and bottom faces, and a plunging axis. Having placed this body beneath the center of the anomaly and inverted for intensity and direction of magnetization to achieve an approximate fit to the data, a subsequent inversion set free all spatial parameters together with intensity and direction of resultant magnetization. The computed TMI imaged in Figure 5 is the sum of the anomaly from this magnetization model with the estimated background field, which together closely match the measured field.

Additional inversions were performed independently (other than using the same estimated background field and identical assumptions of homogeneous magnetization) for a polygonal-section plunging pipe, and (with completely different forward modelling algorithms) for tabular and ellipsoid sources. The four different inversions all match the input data very closely, with no clear grounds from data misfit to favor any one of the models over the others. The models are shown in perspective view in Figure 6. All four have similar centroids, revealing that inversion was able to consistently locate a best-estimate center of magnetization despite the imposed differences in shape. The different bodies overlap considerably, but do display substantial variation in size (particularly between the ellipsoid and other models). Insensitivity to size is to be expected, because as compact bodies behave similarly to a spherical distribution of magnetization, for which there is no sensitivity to size. Volume and intensity of magnetization of the different models are cross-plotted in Figure 7. Despite their wide range in volume and magnetization intensity, all four models have similar magnetic moments of just less than 1.6 x10^{11} A/m.

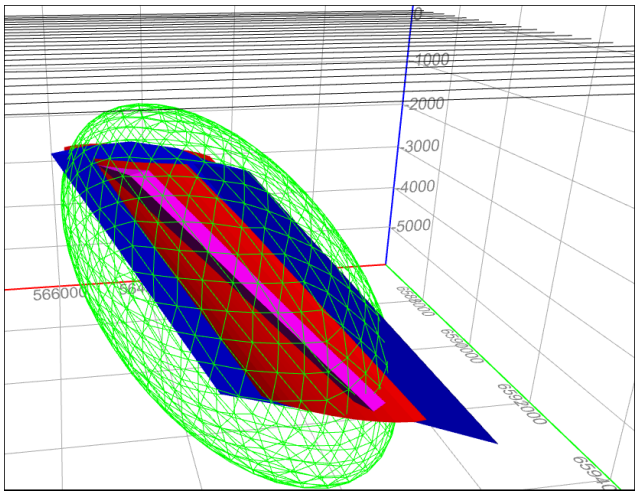

Figure 6: Perspective view of the alternative ellipsoid, tabular and elliptic and polygonal pipe models

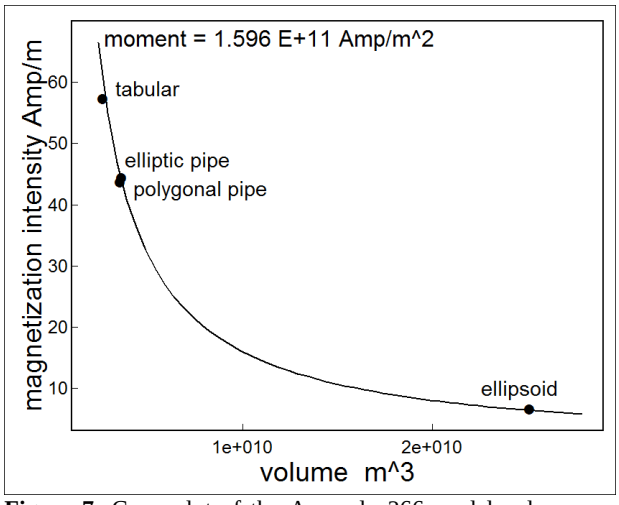

Figure 7: Cross-plot of the Anomaly 266 model volumes and magnetization intensities.

As a consequence of the bodies having similar centers but different volumes, there is also variation in depth to their tops. In contrast, the four model magnetization directions plotted in Figure 8 are almost identical, with a maximum difference of 3°. These estimates are all derived from the same data, with the same assumption of homogeneous magnetization, so that this clustering of directions may overestimate the precision of the estimated magnetization direction. Even so, this consistency may appear surprising, given the skepticism which has prevailed until recently about the ability to recover magnetization direction from magnetic field data. I believe that this consistency arises primarily because magnetization direction is a bulk property, and for compact sources change in estimated magnetization direction is only poorly compensated by changes in the other model parameters. Shape and depth to top are however better visualized as details, and there is only low sensitivity to their estimates due to the ease with which a variation can be compensated by adjustment of other source parameters. Just as there is little to no sensitivity to differences between the various parametric shapes shown in Figure 6, any compact voxel model should provide a similar estimate of magnetization direction and also suffer identically from insensitivity to shape.

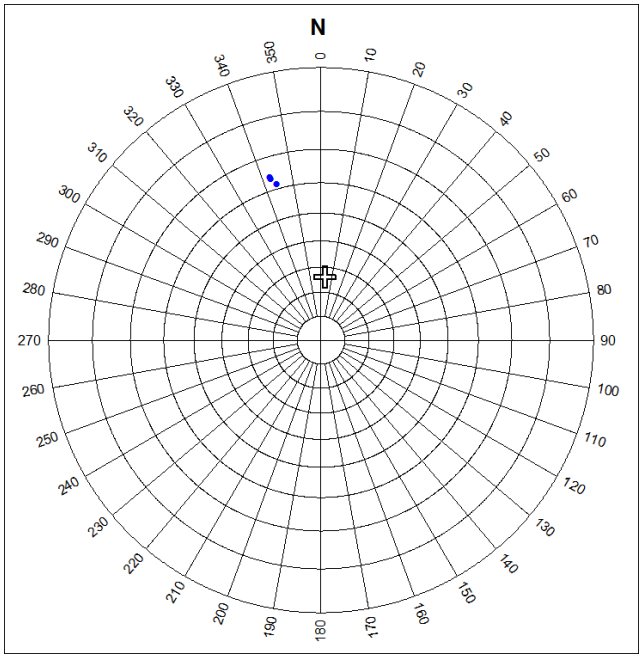

Figure 8: Stereonet plot of the four alternative inversion model magnetization directions. The cross shows the geomagnetic field direction (opposite hemisphere).

A CASE STUDY SENSITIVITY TEST OF MAGNETIC FIELD INVERSION

Anomaly 275 to the south of the main anomaly (Area ‘B’ in Figure 3) is imaged in greater detail in Figure 9. This anomaly has an amplitude of between 800 and 850 nT, and a diameter of 1200 to 1400 m. This is one of the sharpest anomalies due to the reverse remanent magnetization within the survey area, and most probably one of its shallowest occurrences. For this reason

it has been selected for drill testing as part of the Geological Survey of South Australia PACE Frontiers program. Use of an incorrect magnetization direction has historically been one of the reasons why planned drill intersections are not realized. This has generally been because of failure to recognize that the magnetization direction is different to local geomagnetic field direction and deal with it appropriately. A carefully conducted inversion to address the recognized challenge of unknown magnetization direction is more likely to be successful, but it is still important to justify any proposed drill site.

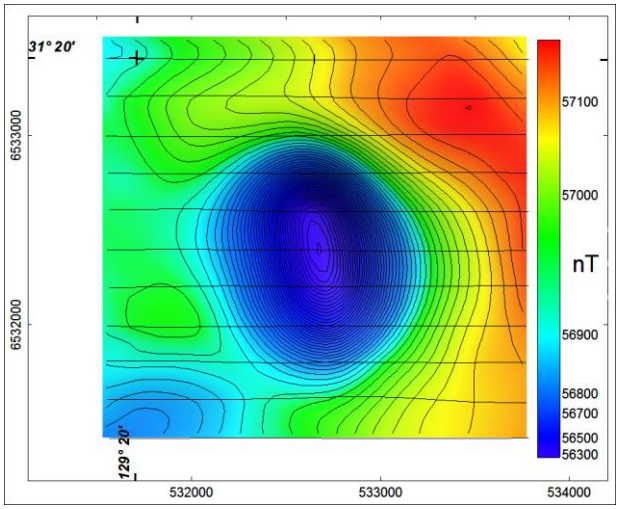

Figure 9: TMI image of Anomaly 275 (area 'B' in Figure 3).

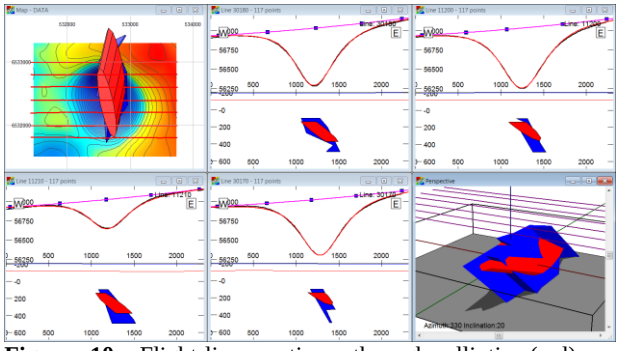

Figure 10: Flight-line sections through elliptic (red) and polygonal (blue) section sheet inversion models.

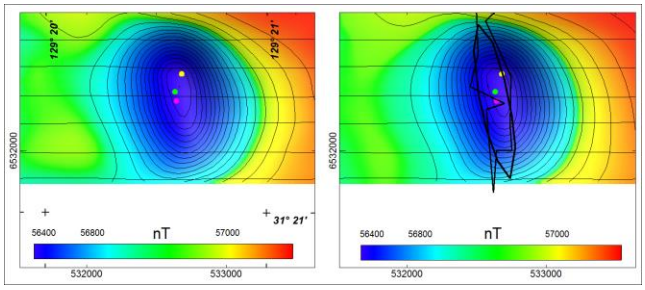

Figure 11: Anomaly 275 measured (left) and computed (right). Green point - peak total gradient; purple - peak NSS, yellow - peak RTP.

A study to support selection of this drill site and to design a borehole trajectory is described by Foss et al. (2016b). The anomaly was inverted using elliptic and polygonal section plunging bodies. Initially these were given almost circular section, but in both cases the inversions elongated the source models in a north-south direction to generate thin sheets which plunge steeply to the east, as shown in Figure 10. At present little is known of the basement geology (Wise et al., 2016) and there is no clear geological grounds to prefer either a pipe or sheet model. As for Anomaly 266, the inversions are successful in matching the input data. Depth to the top of the two models are 254 and 215 m below ground (339 and 300 m below sensor), with a difference of 12% of depth below sensor. The close fit of measured and model computed TMI is shown in Figure 11. Also plotted on Figure 11 are analytic estimates of the center of magnetization given by the peaks of the total gradient transform, the normalized source strength, and RTP (the latter using the magnetization direction derived from the inversions). These points are all consistent with the tops of the inversion models, with displacements between the points mostly along the long axis of the body. The estimated thickness of the sheet is 200 m, but this is poorly constrained (because of effective trade-off between thickness and intensity of magnetization). The proposed drill site on line 11200 (as shown in Figure 12) should penetrate the magnetized body towards the center of its top surface, and sample much of the sheet, including its western contact with the surrounding rock.

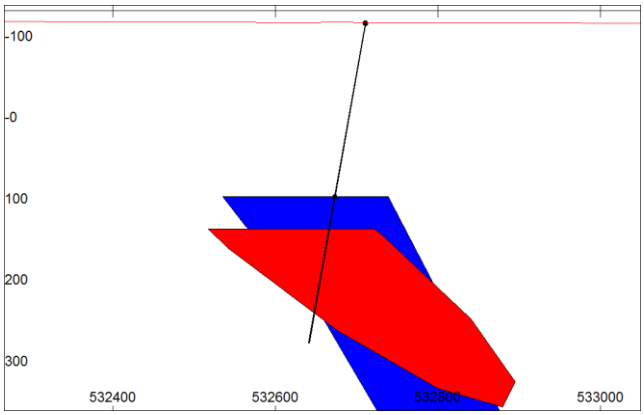

Figure 12: Proposed drill section on Line 11200.

The magnetization direction of the two best-fit inversion models as plotted in Figure 13 are: declination 002°, inclination +24°, and 001°, +23° respectively (a difference of less than 2°). As for Anomaly 266, this very tight clustering is likely to overestimate the true resolution of magnetization direction. Better understanding of confidence in the models can be gained by mapping sensitivity to critical model parameters. To do this, magnetization directions of the two models were offset at 10° intervals to 40° higher and 40° lower declination and inclination, as plotted in Figure 13. A separate inversion of each model was performed at each of these offset magnetization directions, and the post-inversion data misfit was recorded. The post-inversion misfit statistics plotted in Figure 14 confirm that the same best (lowest data misfit) direction is estimated from both models. For an unknown reason the two models show different sensitivities to an anticlockwise (negative) rotation of declination, but both

models have higher sensitivity to reduction of inclination than to increase of inclination (as is generally found). The same misfit statistic, from the same data points, was also derived by offsetting the two models to greater and shallower depths, and inverting to find the best-fit models and their misfit values at those offset depths. These misfit values are also plotted in Figure 14. The horizontal scale in this case is depth rather than angle as for the magnetization direction plots, but the vertical scales are identical. Magnetization direction plays almost no part in compensating for depth variation of the models because these two parameters are poorly linked. Nor does the model have a lower sensitivity to depth because its magnetization is dominated by remanence rather than induction. Compact magnetic sources intrinsically have higher sensitivity to variation of magnetization direction than depth to their top (this is not true for all other shapes, such as extensive planar sheets). As shown in Figure 14, for both of the two models, a variation in magnetization direction of 15° causes a significantly larger increase in data misfit than does a variation in depth to top of 150 m (c.a. 50% of depth below sensor). The main uncertainty of the drill-target model is its depth, rather than its position and dip, which are the factors related to its magnetization direction.

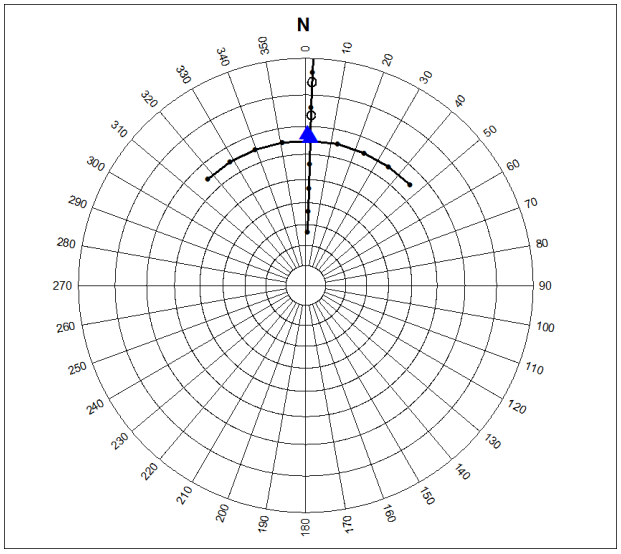

Figure 13: Anomaly 275 model magnetization directions (blue triangles) and sensitivity test directions (open symbols upper hemisphere).

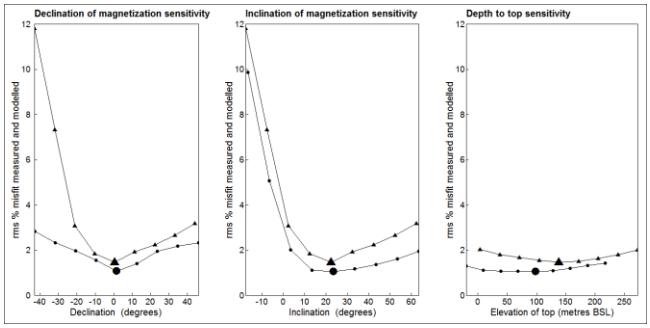

Figure 14: Magnetization sensitivity 'V' curves for declination (left), inclination (center), and depth to top (right). Triangles - elliptic section sheets, circles - polygonal section sheets.

SOLVING FOR COMPLEX MAGNETIZATION DISTRIBUTIONS

Anomalies 266 and 275 are both discrete, well-isolated anomalies which can be explained as due to compact homogeneous magnetizations. Figure 15 shows the southeast satellite anomaly (area 'C' in Figure 3). By visual inspection this anomaly is due to a complex distribution of magnetization, with the likely presence of more than one magnetization direction. There should be no realistic expectation of a 'point and click' inversion solution for this anomaly or complex of overlapping anomalies, but rather, meaningful results are likely to come from interactive decision making and guidance from an interpreter. A study of this anomaly was presented by Foss et al. (2016c).

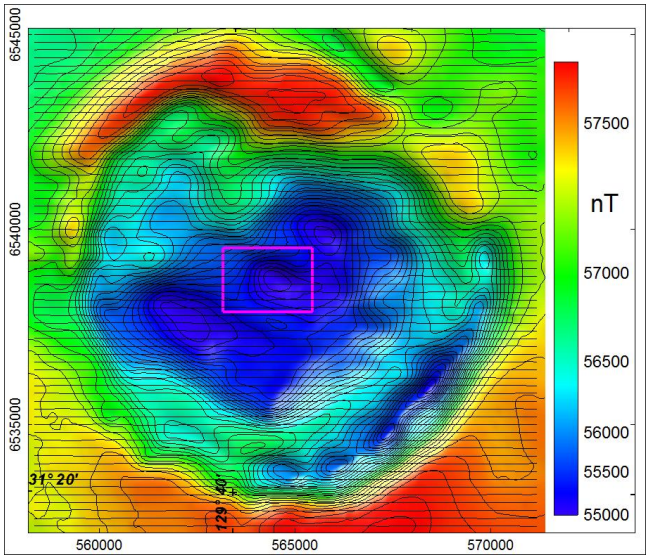

Figure 15: Southeast satellite anomaly TMI.

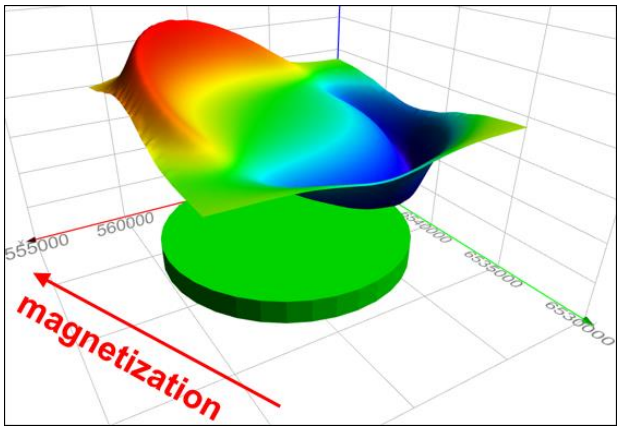

Figure 16: Horizontal polarization concept to explain the normal and reverse anomaly lobes.

Inversion of this anomaly requires careful inspection of the data, to try to reduce the problem to smaller, more manageable tasks. What makes this anomaly different to any of the others in the area is the sharp, high-amplitude dual polarity variation around its margin. The most prominent features are opposite polarity lobes to the northwest and southeast. This orientation is

coincident with the declination of magnetization recovered from some of the discrete anomalies (including Anomaly 266), suggesting that it might possibly be due to a low inclination magnetization of that orientation causing polarization anomalies at either end of the body. Figure 16 shows the field computed from a model to test this concept. The model does indeed create the intended features, but it is difficult to generate the required sharpness of gradient and changes in gradient. While it may be possible to further develop this model, it is worthwhile investigating alternative concepts.

Figure 17 shows a model in which the dual polarity anomalies are generated by dual polarity magnetizations. An acceptable explanation for such a model is that it records a reversal of the main geomagnetic field. Such reversals are well documented as occurring within time spans less than that of a complex or multi-phase intrusion. In this magnetic field reversal model, magnetization is positioned immediately beneath the anomalies, making it easier to generate the sharp gradients required. The field computed from this trial model is compared to the measured anomaly in Figure 18. Clearly the main task remaining is to match the central magnetic low, which is similar to many of the surrounding anomalies.

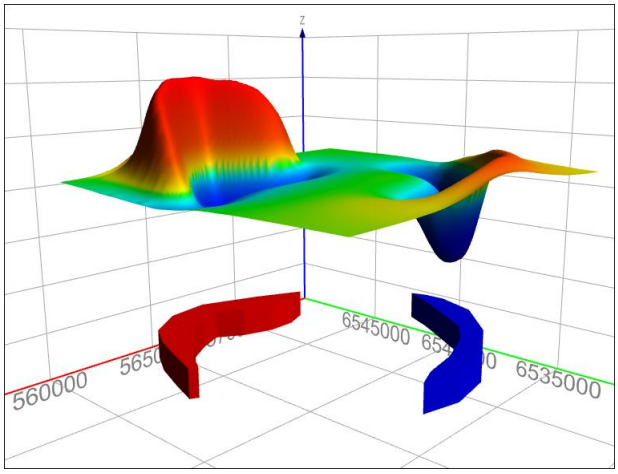

Figure 17: Normal and reverse polarity ring segments concept.

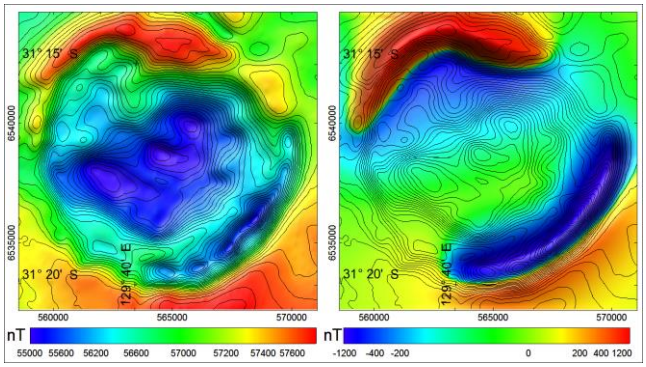

Figure 18: TMI contours on images of (left) measured TMI and (right) TMI computed from the dual polarity ring segments.

The central low is bounded by two steps, which are interpreted to mark the edges of discrete bodies of reverse remanence dominated magnetization. The steps have similar sharpness, so it is not clear whether either magnetization is shallower than the other. Two polygonal bodies were generated, and their perimeter vertices were then adjusted by inversion to match the observed sharp variations in trend of the anomaly margins, together with changes of depth, depth extent, plunge and magnetization intensity and direction. The resulting bodies are shown in Figure 19 (with the surrounding outer ring bodies removed). The inversion has given both bodies a restricted depth extent, so that they appear to be horizontal sheets. The inner body is completely enclosed by the outer body, which is convenient as it means its magnetization can be easily calculated as the vector sum of its own magnetization plus that of the overlapping outer body.

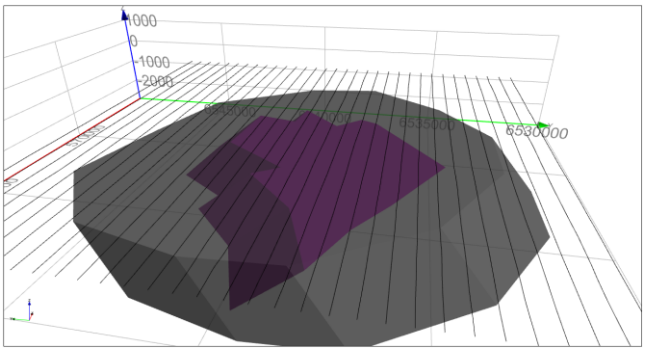

Figure 19: Inner and outer core models added to the outer ring segments to model the anomaly.

Total magnetic intensity computed from the compound model of the double inner zones and the outer ring segments is compared with measured TMI in Figure 20. This figure shows a close fit between the measured and computed fields, with all major features matched. Further adjustment of the model to achieve a closer fit is primarily embellishment or improvement of local detail. The model is shown in plan view in Figure 21, and in perspective view in Figure 22. Note that an additional body has been added at the center of the model to explain a small local anomaly which can be seen in Figures 15 and 20. This body makes such a small contribution to the anomaly that it is very poorly constrained in the complete anomaly inversion. To reduce instabilities with this body I used a circular rather than elliptic section, with a constrained vertical plunge.

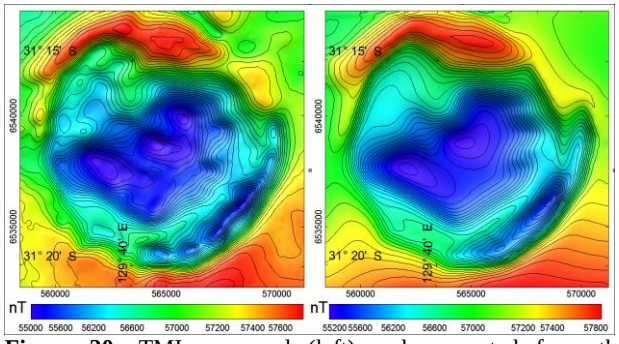

Figure 20: TMI measured (left) and computed from the compound model (right).

Because the outer ring bodies were initially fitted to their specific anomalies and then held constant when the inner zone bodies were added to the model, the final integrated inversion was from a reasonable starting model, and tight constraints could be imposed on movement of the vertex coordinates. This resulted in a final model in which the individual components retained their ascribed task, and combine well to explain the anomaly. An unstructured inversion from a poor starting model would be more likely to create a chaotic model with substantial overlap of bodies. This successful partitioning of a complex model is most easily achieved where there are distinct and sharp gradients in the data to well delineate anomalies. There was no strong case prior to the inversion for imposing any particular geological style to the model, but in this case the inversion model itself is suggestive of a geological interpretation, possibly a volcanic or plutonic complex of limited depth extent.

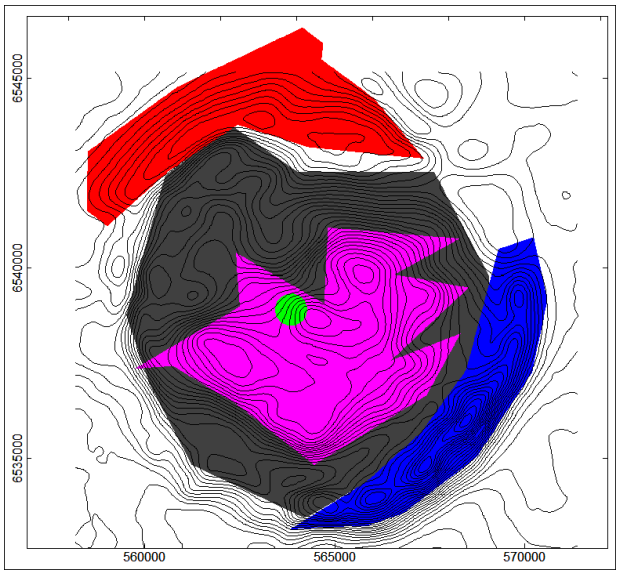

Figure 21: Plan view showing outer ring segments (red and blue), outer and inner core (black and purple), and central (feeder pipe?) (green) with 100 nT interval TMI contours.

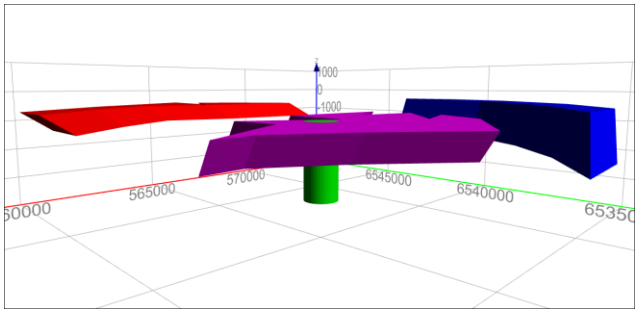

Figure 22: Model perspective view (outer core stripped for simplicity)

Magnetization directions from the various model components are plotted in Figure 23. Closed symbols are lower-hemisphere positive inclinations, and open symbols are upper-hemisphere negative inclinations. The steep inclination, northeasterly directions of the innermost sheet (red circle) and southeast ring segment (red square) are closely grouped, with the northwesterly direction of the intermediate sheet almost 40° away (but similar to several magnetization estimates from other anomalies in the area). The normal magnetization of the northern ring segment (the red open triangle in Figure 23) has a declination 180° from that of the southeast ring segment, but an (opposite polarity) inclination 25° shallower. The fact that these two magnetization directions are not 180° apart does not invalidate the suggestion that they are primarily due to reverse polarity remanences, because these are resultant magnetization directions which include identically directed induced components.

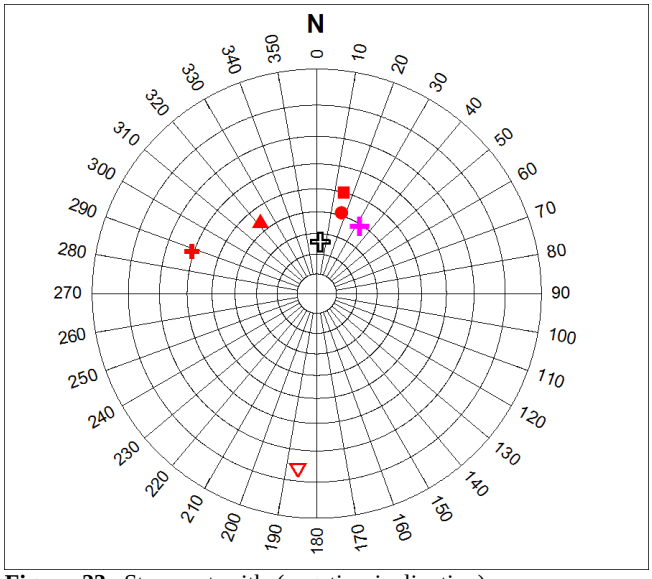

Figure 23: Stereonet with (negative inclination): open cross – geomagnetic field, open triangle – northern ring segment, (positive inclination): red circle – inner zone, red square – SE ring segment, red triangle – intermediate zone, red cross – center pipe from main inversion, magenta cross – center pipe from local inversion.

The 'surplus' magnetization of the central pipe is plotted as the red cross in Figure 23. This body is superimposed on both inner zone bodies, and so all three magnetizations should be summed to give its total magnetization, but I wanted to investigate the contribution of that separate body to the inversion, which is determined by its surplus magnetization. That surplus magnetization direction is not easily explained, and is most likely an artefact of including a body of such slight contribution in the inversion. The central anomaly is poorly resolved in the TMI, but is more clearly expressed in the total gradient transform, imaged in Figure 24, which highlights intense shallow magnetizations.

The central anomaly provides one of the better opportunities within the main anomaly to estimate a depth, and as such it was selected as the site of a possible drill hole. As noted, the body is poorly constrained in inversion of the complete anomaly. The inset boxes in Figures 15 and 24 show the extent of a subset of TMI data which was independently inverted to obtain a more reliable model. Flight-line sections through the model are shown in Figure 25. Anomaly separation is a challenge and a

significant source of uncertainty in the resulting inversion. The best-estimated depth below surface to the magnetization is just over 400 m (but this is poorly constrained). The best estimated direction of the magnetization contrast of this body against the surrounding material (its surplus magnetization) is declination 033°, inclination +51°, which is plotted as the magenta cross in Figure 23. This magnetization direction is only 12° from those of the inner zone and the southeast ring segments, and is interpreted to be an improved estimate of magnetization from the much sharper focus of inverting only the relevant data selection.

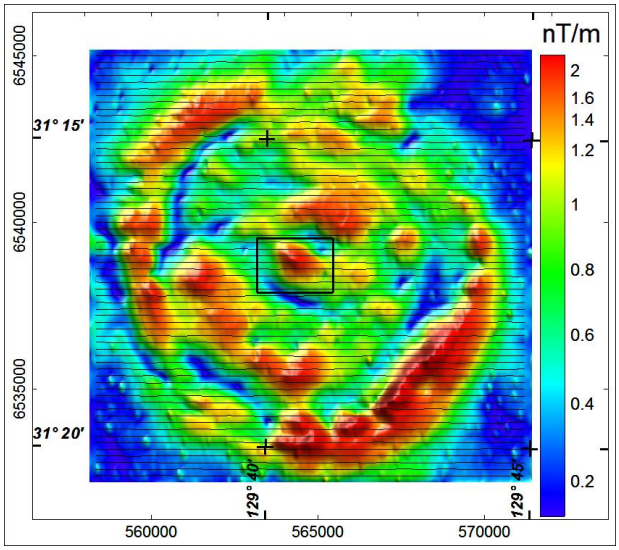

Figure 24: Total gradient of TMI. Inset shows area of central model.

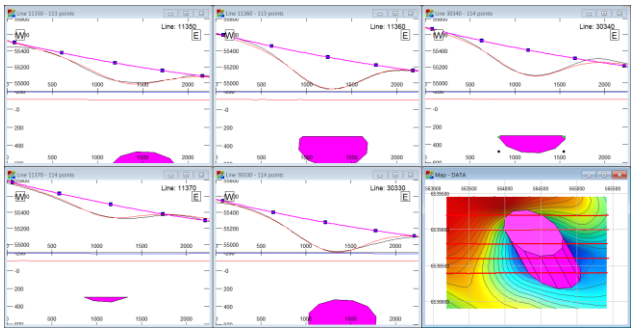

Figure 25 Flight-line sections through the central body model.

A RECOMMENDED APPROACH TO ADRESSING REMANENT MAGNETIZATION IN MAGNETIC FIELD INTERPRETATION

Rock magnetic studies generally reveal remanent magnetizations broadly similar in strength to induced magnetizations (e.g. Dunlop et al., 2010), with the spectrum of induced to remanent magnetization ratios extending up to Koenigsberger ratios >10 (particularly for rocks with lamellar magnetism, e.g. Robinson et al. 2004; Schmidt et al. 207). These results suggest that at least some rotation of magnetization direction away from the geomagnetic field is likely to be the norm, rather than a special case. Possible distributions of apparent resultant rotation angles for populations of sources of magnetic anomalies are plotted schematically in Figure 26. The details of any specific distribution would depend on the ages and magnetic characteristics of the rocks present. Unfortunately, with uncertainties of probably at least 5° on recovering magnetization direction from the most suitable anomalies, it may rarely be feasible to map such distributions from magnetic field studies. Nevertheless, given these expected distributions, perhaps the most appropriate approach to inversion of magnetic field data is not to make a special case of allowing freedom of magnetization direction only where it seems essential, but of asking in all instances why an inversion should not allow freedom of magnetization direction.

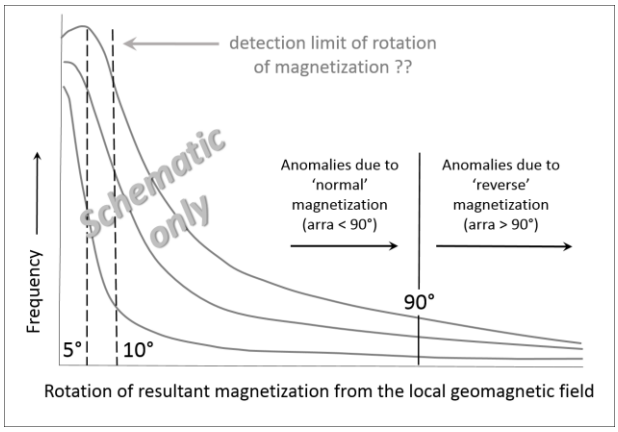

Figure 26: Schematic of populations of differences of magnetization direction from the local geomagnetic field (ARRA) for magnetic anomaly sources.

All magnetic field inversions, by whatever methodology, are attempts to find optimum solutions of multi-parameter systems. Constraint by imposing the known value of any one parameter improves the estimates of all remaining values, but with the danger that imposing an incorrect value may instead degrade the remaining parameter estimates. A solution to this quandary (at least for anomalies due to compact magnetizations) is to invert data twice, once with an induction-only magnetization direction, and separately allowing a free magnetization direction. Preparation of data is a substantial part of most magnetic field inversions, and once that has been done there is only minor additional effort required to run multiple inversions. Furthermore, if the direction of a magnetization is not substantially different to the local geomagnetic field orientation, then inversion allowing a free magnetization direction should still estimate that direction reliably, with the advantage that the magnetization direction is then tested and qualified, rather than just assumed. As shown by Figure 3, it is unlikely that an inversion for a compact magnetization can find an acceptable alternative solution with a substantially different magnetization direction.

Because of the increase in degrees of freedom, inversion with free magnetization direction should always produce a reduced data misfit (although not invariably with a valid improvement of the model). Any substantial reduction of data misfit using a different source magnetization requires explanation, with the

first question being whether that model is geologically acceptable. An unanticipated solution should be questioned, even if it provides a significant improvement in matching the data. Conversely, there will be serendipitous occasions when inversion with a free magnetization direction provides an unanticipated breakthrough in interpreting the data. If two or more models with different magnetization directions provide similar fits to the data, and there are no strong grounds to favor one model over the other, then both those models should be accepted as alternative possibilities (ideally with proposal of a test to discriminate between them). The generation, display and storage of inversion models has become so convenient and rapid that multiple models to explore parameter space should be the norm, with generation of best induced-only and best remanent-also models only the minimum example of a multi-solution output. Many Bayesian inversion schemes utilize multiple minor perturbations of models to explore model space in a probabilistic manner (eg. Lindsay et al., 2013). This approach is also valid to use with perturbation of magnetization direction. Allowing variation of magnetization direction also opens up distant regions of model space which are not readily explored by successive minor changes to a starting model of fixed magnetization direction.

Given the dependence on body shape in recovering estimates of magnetization direction, it is worthwhile trying to quantify a shape factor. As a distribution of magnetization progressively differs from a homogeneous sphere, shape has an increasing influence on any estimates of magnetization derived from magnetic field analysis or inversion. The effect of shape also depends on distance at which the field is measured. For measurements at ever greater distances from a body the influence of its shape diminishes, to the point that it eventually appears to be a dipole, and if the field is still sufficiently defined at that distance, its analysis should provide a robust estimate of magnetization direction. Bodies up to a ratio of 2:1 for maximum elongation (measured as the maximum straight-line distance between two points in the body) to the closest approach at which the magnetic field is measured or computed, act almost identically to a dipole magnetization, regardless of their exact shape. Departure of the measured field from that of a dipole beyond this limit is gradual, and may be of small significance up to values of 8 or more. In this study consistent magnetization directions were derived from quite different shape sources for Anomaly 266, for which the ellipsoid source has a maximum extent to minimum distance to measurement ratio of over 6 (the other bodies have ratios of over 3), and for Anomaly 275 both bodies have a ratio of over 5.

CONCLUSIONS

Case studies in the Coompana area of South Australia show that consistent estimates of magnetization direction and center of magnetization can be recovered by careful inversion of well-isolated magnetic field anomalies over compact magnetizations, regardless of the details of source geometry. A study of a complex distribution of multiple magnetization directions from the same area illustrates that such complexity can be addressed, but this requires a more interactive approach to solve the problem in parts.

ACKNOWLEDGMENTS

The case studies presented in this paper are from a joint Geological Survey of South Australia (GSSA) and CSIRO study funded as part of the PACE Frontiers Program. The magnetic field data are available for download from the GSSA SARIG website: http://www.minerals.statedevelopment.sa.gov.au/online_tools/free_data_delivery_and_publication_downloads/sarig and the magnetization models can be downloaded from the Australian Remanent Anomalies Database, which can be accessed via a link at: https://confluence.csiro.au/display/cmfr/Home . I would like to acknowledge discussions with my GSSA colleagues in this project; Gary Reed, Rian Dutch, Tom Wise, Philip Heath and Tim Keeping. The inversions presented in this paper were generated with ModelVision from Tensor Research, and many of the images were created in Discover PA from Pitney Bowes. I have benefitted from many discussions on remanent magnetization and inversion with former colleagues at Encom Technology (now Tensor Research), namely Blair McKenzie, David Pratt, Tony White and Sam Roberts, and with colleagues in CSIRO, namely Phil Schmidt (now at Magnetic Earth), Jim Austin and David Clark. This paper was substantially improved following a review by Jim Austin.

REFERENCES

Austin, J.R., and C.A. Foss, 2014, The paradox of scale: reconciling magnetic anomalies with rock magnetic properties for cost-effective mineral exploration: Journal of Applied Geophysics, 104, 121-133.

Beiki, M., D.A. Clark, J.R. Austin, and C.A. Foss, 2012, Estimating source location using normalized magnetic source strength calculated from magnetic gradient tensor data: Geophysics, 77, J23–J37.

Clark, D.A., 2012, New methods for interpretation of magnetic vector and gradient tensor data 1: eigenvector analysis and the normalized source strength: Exploration Geophysics, 43(4), 267-282.

Clark, D.A., 2013, New approaches to dealing with remanence: magnetic moment analysis using tensor invariants and remote determination of in situ magnetisation using a static tensor gradiometer: ASEG Extended Abstracts 2013, 1–7.

Clark, D.A., 2014, Methods for determining remanent and total magnetisations of magnetic sources – a review: Exploration Geophysics, 45, 271-304.

Dannemiller, N., and Y. Li, 2006, A new method for determination of magnetization direction: Geophysics, 71, L69–L73.

Dunlop, J.D., O. Özdemir, and V. Costanzo-Alvarez, 2010, Magnetic properties of rocks of the Kapuskasing uplift (Ontario, Canada) and origin of long-wavelength magnetic anomalies: Geophys. J. Int., 183, 645-658.

Ellis, R. G., B. de Wet, and I.N. Macleod, 2012, Inversion of magnetic data for remanent and induced sources: ASEG Extended Abstracts 2012, 1–4.

Fedi, M., G. Florio, and A. Rapolla, 1994, A method to estimate the total manetization direction from a distortion analysis of magnetic anomalies: Geophysical Prospecting, 42, 261-274.

Foss, C.A., 2006, Evaluation of strategies to manage remanent magnetization effects in magnetic field inversion: 76th Annual International Meeting, SEG, Expanded Abstracts, 938–942.

Foss, C.A., and K.B. McKenzie, 2009, Strategies to invert a suite of magnetic field anomalies due to remanent magnetization: an example from the Georgetown area of Queensland: ASEG Extended Abstracts 2009, 1–18.

Foss, C.A., and B. McKenzie, 2011, Inversion of anomalies due to remanent magnetisation: An example from the Black Hill Norite of South Australia: Australian Journal of Earth Sciences, 58, 391–405.

Foss, C.A., G. Reed, T. Keeping, T.W. Wise, and R.A. Dutch, 2016a, Looking into a 'blue hole' – resolving magnetization and structure from the complex negative Coompana anomaly, South Australia: ASEG Extended Abstracts 2016, 1-8.

Foss, C.A., G. Reed, T. Keeping, T.W. Wise, and R.A. Dutch, 2016b, Model sensitivity studies to support drill tests of buried remanent magnetization in the Coompana area, South Australia: Near Surface Geoscience – First Conference on Geophysics for Mineral Exploration and Mining, Extended Abstracts, 1-8.

Foss, C.A., G. Reed, T. Keeping, T.W. Wise, and R.A. Dutch, 2016c, Inversion of an anomaly due to multiple magnetizations: An example from the Coompana survey, South Australia. SEG Technical Program Expanded Abstracts 2016: pp. 1511-1515. doi: 10.1190/segam2016-13972845.1

Fullagar, P. K., and G. A. Pears, 2015, Remanent magnetisation inversion: ASEG Extended Abstracts 2014.

Heath, P., G. Reed, and L. Katona, 2015, 2015 Coompana airborne survey: MESA Journal, 79(4), 18-21.

Helbig, K., 1963, Some integrals of magnetic anomalies and their relation to the parameters of the disturbing body: Zeitschrift für Geophysik, 29, 83–96.

Lelièvre, P. G., and D. W. Oldenburg, 2009, A 3D total magnetization inversion applicable when significant, complicated remanence is present: Geophysics, 74 (3), L21–L30.

Li, Y., S. Shearer, M. Haney, and N. Dannemiller, 2010, Comprehensive approaches to the inversion of magnetic data affected by remanent magnetization: Geophysics, 75, L1–L11.
Li, Y., 2012, Recent advances in 3D generalized inversion of potential-field data: 82nd Annual International Meeting, SEG, Expanded Abstracts, 1–7.

Lindsay, M.D., S. Perrouty, M.W. Jessell, and L. Ailleres, 2013, Making the link between geological and geophysical uncertainty: geodiversity in the Ashanti Greenstone Belt: Geophys, J. Int., 195, 903-922.

MacLeod, I.N., and R.G. Ellis, 2013, Magnetic vector inversion – a simple approach to the challenge of varying direction of rock magnetization: A Forum on the Application of Remanent Magnetisation and Self Demagnetisation Estimation to Mineral Exploration: ASEG Extended Abstacts 2013.

Macnae, J., 1994, Viscous magnetization: misleading Koeningsberger's Q: 64th Annual International Meeting, SEG, Expanded Abstracts, 456–458.

McEnroe, S.A., P. Robinson, N. Miyajima, K. Fabian, D. Dyar, and E. Sklute, 2016, Lamellar magnetism and exchange bias in billion-year-old titanohematite with nanoscale ilmenite exsolution lamellae: I. Mineral and magnetic characterization: Geophys. J. Int., 206, 470-486.

Paine, J., M. Haederle, and M. Flis, 2001, Using transformed TMI data to invert for remanently magnetised bodies: Exploration Geophysics, 32, 238–242.

Phillips, J., 2005, Can we estimate total magnetization directions from aeromagnetic data using Helbig's formulas: Earth Planets Space, 57, 681–689.

Phillips, J. D., M.N. Nabighian, D.V. Smith, and Y. Li., 2007, Estimating locations and total magnetization vectors of compact magnetic sources through combined Helbig and Euler analysis: 77th Annual International Meeting, SEG, Expanded Abstracts, 770–774.

Pilkington, M., and M. Beiki, 2013, Mitigating remanent magnetization effects in magnetic data using the normalized source strength: Geophysics, 78 (3), J25–J32, doi: 10.1190/geo2012-0225.1.

Pratt, D. A., K.B. McKenzie, and A.S. White, 2014, Remote remanence determination (RRE): Exploration Geophysics, 45, 314-323.

Rajapgopalan, S., P.W. Schmidt, and D.A. Clark, 1993, Rock magnetism and geophysical interpretation of the Black Hill Norite, South Australia: Exploration Geophysics, 24, 209-212.

Robinson, P., R.J. Harrison, S.A. McEnroe, and R.B. Hargraves, 2004, Nature and origin of lamellar magnetism in the hematite-ilmenite series: The American Mineralogist, 89, 725–747.

Roest, W. R., J. Verhoef, and M. Pilkington, 1992, Magnetic interpretation using the 3-D analytic signal: Geophysics, 57, 116–125.

Roest, W., and M. Pilkington, 1993, Identifying remanent magnetization effects in magnetic data: Geophysics, 58, 653–659.

Schmidt, P.W., D.A. Clark, and S. Rajagopalan, 1993, An historical perspective of the Early Palaeozoic APW of Gondwana: new results from the Early Ordovician Black Hill Norite of South Australia: Exploration Geophysics, 24, 257-262.

Schmidt, P.W., and D.A. Clark, 1997, Directions of magnetization and vector anomalies derived from total field surveys: Preview, 70, 30-32.

Schmidt, P.W., and D.A. Clark, 1998, The calculation of magnetic components and moments from TMI: a case study from the Tuckers igneous complex, Queensland: Exploration Geophysics, 29, 609–614.

Schmidt, P. W., S.E. McEnroe, D.A. Clark, and P. Robinson, 2007, Magnetic properties and potential field modeling of the Peculiar Knob metamorphosed iron formation, South Australia: an analog for the source of the intense Martian magnetic anomalies?: Journal of Geophysical Research, 112, B03.

Wise, T.W., M.J. Pawley, and R.A. Dutch, 2016, Preliminary interpretations from the 2015 Coompana aeromagnetic survey: MESA Journal 79(4), 22-30.